Noninvasive assessment of coronary stents in patients by 16-slice computed tomography

【structured abstract】

Background: The usefulness of thin-slice mult-detector computed tomography (MDCT) has been highly expected to assess the lumens of coronary artery stents. We evaluated the usefulness of 16-slice MDCT to assess the in-stent lumen after coronary artery stenting. *Methods:* In 42 consecutive patients after coronary artery stenting, retrospective ECG-gated CT-angiography using 16-slice MDCT (0.5sec rotation time, 16 ×0.625-mm detector collimation) was performed. The qualitative assessability of the lumens of 61 coronary stents (14 different types) by MDCT and the reasons for nonassessability were investigated. Furthermore, the evaluation of in-stent restenosis in 21 assessable stents of 16 patients, including quantitative density analysis by MDCT, was performed and the results were compared with those of conventional coronary angiography (CAG). *Results:* Of 61 stents, 42 (68.9%) were assessable. The assessability of diameter≥3.5-mm stents made of stainless steel or cobalt was high (88.6%, 31/35), that of 3.0-mm stents was low (57.9%, 11/19) and all 2.5-mm stents were non-assessable due to partial volume effects and metal artifacts of stents. The lumens of stents made of tantalum were totally obscured and the metal artifacts of Bestent2 (gold markers) and S670 were severer than others. All non-assessable stents due to banding artifact and calcification were implanted in segment #1-3 and #6, respectively. In comparison to CAG, MDCT correctly detected the 5 in-stent restenoses and identified absence of restenosis in the remaining 16 stents. The quantitative density analysis of in-stent restenoses was influenced strongly by the stent strut. *Conclusion*: Despite some limitations, 16-slice MSCT is sufficiently useful for assessment of various coronary stents in patients and can detect in-stent restenoses of assessable stents with high accuracy in comparison to CAG.

【key words】 Coronary stent; Restenosis; MDCT

1. Introduction

The introduction of multi-detector computed tomography **(MDCT)** permitted visualization of coronary arteries with reasonable temporal and spatial resolution using electrocardiogram **(ECG)**-gated CT-angiography and MDCT has been applied to the new method for assessment of coronary arteries [1-5], coronary artery plaques [6, 7] and bypass grafts [8]. In addition, a new generation of MDCT scanners, equipped with more and thinner detector rows and increased rotation speed, has been recently introduced, and therefore the usefulness of MDCT to assess the lumens of coronary artery stents (the presence or absence of in-stent restenosis) has been also highly expected. In the report about carotid stents, MDCT allows accurate analysis of the relationship between the stent and the vessel lumen [9], while 4-slice MDCT allows no direct visualization of coronary in-stent restenosis due to partial volume effects and beam hardening (the metal artifacts of stents), therefore a reliable evaluation of in-stent restenosis dose not seem practical by 4-slice MDCT [10, 11]. In this study, we investigated the ability of 16-slice MDCT for visualization of various coronary artery stents in patients and the

reasons for non-assessable images. In addition, we examined the accuracy of 16-slice MDCT in detecting coronary stent restenosis in comparison to conventional coronary angiography.

2. Materials and methods

2.1. Patients and coronary artery stents

Sixteen-slice MDCT was performed in 42 consecutive patients (32 males, aged 66.2 ±8.4 years, body mass index 23.5±2.2 kg/m^2) at a mean interval of 14.0±18.3 months (range 1 to 60 months) after coronary stent implantation. In these patients, a total of 61 stents (14 different stent types) were implanted. The details of each stent type were summarized in **Table 1**. Exclusion criteria included (1) irregular heart rate (chronic atrial fibrillation, frequent premature beats, and so forth), (2) renal dysfunction (serum creatinin＞1.5mg/dl), (3) allergy to contrast media, (4) severe deafness (breath hold is impossible) and (5) unstable hemodynamic situation. The study was approved by the hospital's ethical committee and informed consent was obtained from all patients.

2.2. MDCT scan protocol

Helical CT-angiography using 16-slice MDCT (LightSpeed Ultra16. GE Healthcare, Wisconsin; gantry rotation time 0.5sec, 16 × 0.625-mm detector collimation) was performed under the retrospective ECG-gated method. Of 42 patients, 38(heart rate at rest ≥60bpm, 90.5%) received 40mg metoprolol (Seroken™, AstraZeneca PLC, London, United Kingdom) orally 60min before MDCT scanning, and all received 0.3mg nitroglycerin (Myocolspray™, ToaEiyo Ltd., Tokyo, Japan) sublingually 5min before MDCT scanning. A plain localization scan that yielded an anteroposterior view of the chest was performed to decide the position (z axis coverage) of the imaging volume for coronary arteries imaging. After imaging at the level of the left ventricular, the region of interest was positioned in the cavity of the left ventricular. In 17 cases of all the 42 patients, a bolus of 100 ml of the contrast medium (iohexol 300 or 370mgI/ml, Schering AG, Berlin, Germany) was injected into the right cubital vein at 2.5-4.0 ml/s, followed by a saline chaser bolus of 60 ml at 3.0 ml/s (dual shot™, NemotoKyorindou Co. Ltd., Tokyo, Japan), and as soon as the monitored signal density of the region of interest reached a predefined threshold of 100 Hounsfield units, the scan was started (Smart prep™, GE Healthcare). In the remaining 25 cases, first, a bolus of 5 ml of the contrast medium was injected into the right cubital vein at 3.5 ml/s, followed by a saline chaser bolus of 15 ml at 3.5 ml/s and the time interval between contrast agent injection and the maximum enhancement within the region of interest was measured. Next, a bolus of 90ml of the contrast medium was injected into the right cubital vein at 3.5ml/s, followed by a saline chaser bolus of 20ml at 3.5ml/s and the scan was started with a delay according to the previously determined contrast transit time (test injection method). Image acquisition was performed during an inspiratory breath hold without inhalation of oxygen. The volume data sets were acquired in spiral mode, with simultaneous acquisition of 16 parallel slices (slice thickness 0.625-mm, gantry rotation time 0.5 to 0.6sec, helical pitch 0.275 to 0.325:1, table feed 2.75 to 3.25-mm/rotation, tube current 350 to 400 mAs, tube voltage 120 to 140 kV). The patient's ECG was digitized and continuously monitored during scanning.

2.3. Image reconstruction:

The raw data of the scans were transferred to a computer workstation (Advantage Workstation Ver.4.05, GE Healthcare) and the image reconstruction was performed using image analyzing software (CardIQ Ⅰ or Ⅱ ™. GE Healthcare). According to the heart rate during scanning, half reconstruction algorithm (heart rate ＜65bpm, 1 sector, temporal window 250ms) or multi-sector reconstruction algorithm (heart rate ≥65bpm, 2 to 4 sectors, temporal window ≤125ms) was selected. Initially, volume rendering images of the 20 phases were created at an interval of 5% from the beginning (0%) to the end (95%) of the cardiac cycle (R-wave to R-wave interval), with a slice thickness of 1.25-mm, and the phase with the fewest motion artifacts was chosen. Next, the data sets of the phase with the fewest motion artifacts was reconstructed by volume rendering and curved multiplanar reconstruction methods, with a slice thickness of 0.625-mm. In each patient, the phase with the fewest motion artifacts was used for further evaluation for the left coronary artery and right coronary artery respectively.

2.4. MDCT image evaluation

On the basis of the axial, oblique, volume rendering and curved multiplanar reconstruction images, the image quality of each coronary artery stent was judged by the agreement of 3 observers (a radiological technologist and two cardiologists) as sufficient or insufficient for patency and in-stent restenosis evaluation. The stent was considered to be assessable, when the stent lumen was visible and the contrast density of the lumen could be evaluated qualitatively without the influence of partial volume effects, metal artifacts of stents (beam hardening, severe streak artifact and undershooting artifact), cardiac motion artifacts (banding artifacts) and calcification in the arterial wall. In all patients, each coronary artery stent visualized with the MDCT images was divided into two groups (assessable or non-assessable group), and the reasons for nonassessablity ((A) partial volume effects and metal artifacts of stents, (B) banding artifacts, (C) calcification) were investigated. When the judgment varied among the observers, the agreement of 2 observers was selected.

2.5. Detection of in-stent restenosis

In 16 cases of all the 42 patients, in which conventional coronary angiography was performed within 4 weeks after MDCT, the presence or absence of in-stent restenosis in each coronary stent visualized with the MDCT images and divided into assessable group (21stents) was evaluated by the preceding 3 observers. In-stent restenosis was considered to be present, when the vessel distal to the stent implantation site was not visualized (occlusion) or massive low density area in the stent lumen was detected visually as compared with the reference vessels (the sites proximal and distal to the stent). In addition, the CT numbers (Hounsfield units) of at least 5 regions of interest (each region area ＜1mm^2) positioned in the low density area were measured using the software (CardIQ Ⅰ or Ⅱ ™) and the minimum value of those was decided as the CT number of the low density area. In-stent restenosis was considered to be absent, when the contrast density in the stent lumen was almost homogeneous and similar to the density in the reference vessels visually. When the assessment varied among the observers, the agreement of 2 observers was selected.

Conventional coronary angiography was evaluated by a blinded reviewer using quantitative coronary angiography (INTEGRIS HM3000, Philips Medical Systems, Netherlands) and the usual gold standard for in-stent restenosis detection. Stenosis ≥50% (50%, 75%, 90%, 99%, 100%, American Heart Association classification) at the

stent implantation site was decided to be in-stent restenosis. These results were compared to those of MDCT.

3. Results

The mean heart rate before the scan was 54.7±7.5 bpm (range: 45 to 83 bpm). The heart rate changed to 56.3±7.8 bpm (range: 46 to 93 bpm) during breath hold. The mean scan time (the mean duration of breath hold) was 21.1±2.4 seconds （20 to 30seconds）. The helical pitch (table feed) determined the scan time and varied among the patients. In all patients, there were no obvious complications of the MDCT scanning.

The results of the assessment of coronary artery stents in patients by 16-slice MDCT were shown in **Table 2**. Of all the 61 coronary stents, 42 (68.9%) were assessable, and 19 (31.1%) were non-assessable because of partial volume effects and metal artifacts of stents (n=11), calcification (n=3) and banding artifacts (n=5). Concerning diameter≥3.5-mm stents made of stainless steel or cobalt, the assessability was high (88.6%, 31/35) and all stents without severe calcification and banding artifacts at the sites of stents implantation were assessable. The lumens of stents made of tantalum were totally obscured and invisible due to the severe metal artifacts. The assessability of 3.0-mm stents was low (57.9%, 11/19) and the metal artifacts of Bestent2 (the gold markers of bilateral edges) and S670 reduced the assessability. All the 2.5-mm stents were non-assessable due to partial volume effects and metal artifacts of stents, regardless of stent types. All the non-assessable stents due to banding artifacts and calcification were implanted in segment #1-3 (American Heart Association classification) of the right coronary artery and segment #6 of the left anterior descending artery, respectively.

In assessable 21 coronary stents of 16 cases in which conventional coronary angiography was performed, in-stent restenoses were present in 5 stents (stenotic rate: ①50%, ②90%, ③99%, ④99%, ⑤100%) and absent in the remaining 16 stents. In MDCT images, the 5 in-stent restenoses were correctly detected and absence of in-stent restenosis was correctly identified in the 16 stents. The CT numbers of the low density areas in the stent lumens varied among the 5 in-stent restenoses (CT number: ①107±6, ②78±9, ③116±5, ④270±7, ⑤75±10; Hounsfield units). **Fig 1** and **2** show the cases in which in-stent restenosis was present. **Fig 3** shows the case in which in-stent restenosis was absent.

4. Discussion

Our study demonstrated that 16-slice MDCT could be sufficiently useful for assessment of various coronary artery stents in patients. In the report about 4-slice MDCT (slice thickness 1.25-mm) [10], multiple difficulties contribute to the inability to visualize the stent lumens: (a) the small diameter of coronary arteries, (b) partial volume effects and beam hardening and (c) cardiac motion artifacts. On the other hand, the recent introduction of 16-slice MDCT scanners (slice thickness 0.625-mm) increased the spatial resolution and made the reconstruction of near-isotropic data sets possible, therefore partial volume effects and the beam hardening of stents were decreased greatly. Moreover, the motion artifacts due to respiration and heart beat which had been the main reason for nonassessability of cardiac CT were also decreased greatly by the shorter scan time of 16-slice MDCT (approximately 20 seconds). In consequence, it is suggested that 16-slice MDCT allows for visualization of coronary artery stents with higher spatial resolution and with less motion artifacts.

However, in our study, it was also suggested that several factors might be influential on the visualization of coronary artery stents in patients by 16-slice MDCT. The grade of metal artifacts of stents including partial volume effects is related to the stent material, the size of the diameter, the thickness and the strut design. The metal artifact of tantalum was very severe in comparison to the other materials, therefore it was considered to be impossible to assess the lumens of the stents made of tantalum by MDCT. Moreover, the severe artifact of the gold marker (Bestent2) made the bilateral edges of the stent lumen evaluation difficult. With respect to the size of the diameter, the partial volume effects and metal artifacts of ≤3.0-mm stents were more influential on the assessability of the stent lumens **(Table 3)** and it was considered to be impossible to assess the lumens of the smallest coronary stents (diameter 2.5-mm) with the spatial resolution of the present MDCT. The metal artifacts of thicker stents are likely to be severer and the metal artifacts of thinner stents are less influential on the assessability of the stent lumens. However, in our study, the assessability of ≥3.5-mm stents made of stainless steel or cobalt by 16-slice MDCT was not affected by the partial volume effects and metal artifacts, regardless of the thickness. In addition, it was considered that the reason for lower assessability of S670 (diameter 3.0-mm) in comparison to the other 3.0-mm stents was the severe metal artifacts attributed to the strut design of S670. This analysis would be suggested more truly in comparison between S670 and Multilink Penta, which had the same material and the almost same thickness **(Table 3)**.

As the patients' factors that might limit proper assessment of the stent lumens as well as the native coronary artery lumens, cardiac motion artifacts (banding artifacts) and severe calcification should be mentioned. Cardiac motion artifacts were more likely to limit proper assessment of the stents implanted in the right coronary arteries (especially in segment #2). Calcification in the proximal portion of the left anterior descending artery was most likely to be severe and it was most influential on the assessability of the stents implanted in segment #6. These effects of the patients' factors are considered to be the limitations of the present MDCT.

Our study also demonstrated that 16-slice MDCT could detect in-stent restenoses of assessable coronary stents with high accuracy in comparison to conventional coronary angiography as gold standard. We used the method of evaluating the contrast condition of stent lumens visually to detect in-stent restenosis. In the report about assessment of coronary artery stents with the profile curves [9], the measured CT number (Hounsfield units) in the stent lumen is influenced strongly by the stent material, the size of the diameter, strut thickness and strut design. In our study, the quantitative density analysis of in-stent restenosis (intimal hyperplasia) found different values among the cases. The CT number in the stent lumen is likely to be overestimated by the partial volume effect of stent strut. Therefore the true CT number of intimal hyperplasia is considered to be our minimum value (75±10 Hounsfield units), corresponding to the CT number of intimal hyperplasia found at the site of a carotid artery stent (75.6±5.6 Hounsfield units) [13], close to that found at the site of the left main coronary stent (88 ±10 Hounsfield units) [14]. However, the quantitative density analysis of the stent lumen with MDCT might be less practical clinically because of its inconstancy and the visual and qualitative assessment of the stent lumen might be the best method for detection of in-stent restenosis with the spatial resolution of the present MDCT. Funabashi et al also reported the case in which the patency of the coronary arterial lumen surrounded by the metallic stent could be evaluated visually without any artifact from the metallic stent in the axial image and cut-plane volume rendering image [15].

Limitations of our study include the relatively small number of stents and the fact that analysis was performed with the same method in all patients, regardless of body weight. The image quality of MDCT is more likely to deteriorate due to small

signal-to-noise ratio in obese patients. This patients' factor might be influential on the result of coronary stents visualization. So the analysis in more stents and classified patients by the body weight may be necessary for more precise investigation of the ability of 16-slice MDCT. In addition, another problem is the high radiation dose of 7 to 10 milli Sievert required for 16-slice MDCT.

Our study suggests the potential of 16-slice MDCT to assess coronary stents and detect in-stent restenosis. At present, CT-angiography using thin-slice MDCT is considered to be the most promising method for noninvasive assessment of in-stent restenosis. The introduction of drug eluting stents is expected to reduce the incidence of in-stent restenosis greatly [16], therefore the establishment of noninvasive and easy assessment of in-stent restenosis using thin-slice MDCT is more desirable. In addition, it is also expected that future improvement in spatial resolution by introducing flat panel detectors (spatial resolution 0.15×0.15-mm) will overcome the limitations of present MDCT and enable more precise assessment of the stent lumen including the assessment of stenotic rate.

Acknowledgments

We express our special thanks to Takayuki Suzuki, Kouichi Fujikawa and Hiroshi Yamaguchi in the Department of Diagnostic Imaging, Hiroshima General Hospital for their technical support, and Tatsuya Nakao in the Department of Cardiovascular Surgery, Hiroshima General Hospital for his assistance with the manuscript.

References

[1] Kachelriess M, Kalender WA. Electrocardiogram-correlated image reconstruction from subsecond spiral computed tomography scans of the heart. Med phys 1998; 25: 2417-2431.

[2] Ohnesorge B, Flohr T, Becker C et al. Cardiac imaging by means of electrocardiographically gated multisection spiral CT: Initial experience. Radiology 2000; 217: 564-571.

[3] Nieman K, Oudkerk M, Rensing BJ et al. Coronary angiography with multislice computed tomography. Lancet 2001; 357: 599-603.

[4] Achenbach S, Giesler T, Ropers D et al. Detection of coronary artery stenosis by contrast-enhanced, retrospectively electrocardiographically-gated, multislice spiral computed tomography. Circulation 2001; 103: 2535-2538.

[5] Knez A, Becker CR, Leber A et al. Usefulness of multislice spiral computed tomography angiography for determination of coronary artery stenosis. Am J Cardiol 2001; 88: 1191-1194.

[6] Schroeder S, Kuettner A, Kopp AF et al. Noninvasive evaluation of the prevalence of noncalcified atherosclerotic plaques by multi-slice detector computed tomography: results of a pilot study. Int J Cardiol 2003; 92: 151-155.

[7] Leber A, Knez A, Becker A et al. Accuracy of multidetector spiral computed tomography in identifying and differentiating the composition of coronary

atherosclerotic plaques. J Am Coll Cardiol 2004;43: 1241-1247.
[8] Burgstahler C, Kuettner A, Kopp AF et al. Non-invasive evaluation of coronary artery bypass grafts using multi-slice computed tomography: initial clinical experience. Int J Cardiol 2003; 90: 275-280.
[9] Leclerc X, Gauvrit JY, Pruvo JP. Usefullness of CT angiography with volume rendering after carotid angioplasty and stenting. AJR Am J Roentgenol 2000; 174: 820-822.
[10] Kruger S, Mahnken HA, Sinha MA et al. Multislice spiral computed tomography for detection of coronary stent restenosis and patency. Int J Cardiol 2003; 89: 167-172.
[11] Maintz D, Grude M, Fallenberg E.M, Heindel W, Fischbach R. Assessment of coronary arterial stents by multislice-CT angiography. Acta Radiologica 2003; 44: 597-603.
[12] Anami K, Anno H, Hayashiguchi A et al. Visualization of coronary artery stents by MSCT at 0.5-mm slice thickness. Jpn. J.Radiol 2003; 60: 278-285.
[13] Cademartiri F, Mollet N, Nieman K, Krestin GP, de Feyter PJ. Neointimal hyperplasia in carotid stent detected with multislice computed tomography. Circulation 2003; 108: e147.
[14] Gilard M, Cornily JC, Rioufol G et al. Noninvasive assessment of left main coronary stent patency with 16-slice computed tomography. Am J Cardiol 2005; 95; 110-112.
[15] Funabashi N, Komiyama N, Yanagawa N, Mayama T, Yoshida K, Komuro I. Coronary artery patency after metallic implantation evaluated by multislice computed tomography. Circulation 2003; 103: 147-148.
[16] Sousa JE, Costa MA, Abizaid A et al. Sirolimus-eluting stent for the treatment of in-stent restenosis: a quantitative coronary angiography and three-dimensional intravascular ultrasound study. Circulation 2003; 107: 24-27.

Figure legends

Fig 1. The case in which in-stent restenosis could be detected by 16-slice MDCT. (a) MDCT volume rendering image shows the right coronary artery including the site of stent implantation. Large arrows indicate the stent (#2, NIR 4.0×25: diameter × length; mm). (b) MDCT curved multiplanar reconstruction image shows the massive low density area in the stent lumen. (c) (the enlarged image of the square area in (b)) The CT number of the low density area is 107±6 Hounsfield Unit (arrow head). (d) Conventional coronary angiography shows in-stent restenosis (50%) (small arrows).

Fig 2. The case in which in-stent restenosis could be detected by 16-slice MDCT. (a) MDCT volume rendering image shows the entire left anterior descending coronary artery clearly. Large arrows indicate Stent-A (#7 proximal site, Multilink Penta 3.0× 15mm) and Stent-B (#7 distal site, S670 3.0×15mm). (b) MDCT curved multiplanar reconstruction image shows the massive low density area in the distal site of Stent-A lumen and the reduction of the contrast density in Stent-B lumen. (c) (the enlarged image of the square area in (b)) The CT numbers of the low density area in the distal site of Stent-A lumen (white arrow head) and the Stent-B lumen (black arrow head) are 116±5 and 270±7 Hounsfield Unit, respectively. d) Conventional coronary angiography shows in-stent restenosis (99%) that extends from the distal site of Stent-A to Stent-B lumen (small arrows).

Fig 3. The case in which absence of in-stent restenosis could be identified by 16-slice MDCT. (a) MDCT volume rendering image shows the entire left anterior descending coronary artery clearly. Large arrows indicate the drug eluting stent (#7 Cypher 3.5× 23mm). (b) In the MDCT curved multiplanar reconstruction image, the metal artifact is relatively severe, but the stent lumen is sufficiently visible. (c) (the enlarged image of the square area in (b)) The contrast density in the stent lumen is almost homogeneous and similar to the density in the sites proximal and distal to the stent visually. (d) Conventional coronary angiography shows the site of stent implantation without stenosis (small arrows).

Table 1
Type of stent, thickness, material, manufacture and implanted coronary segment of the examined stents

Stent type	n	thickness (10^{-4} inch)	material	manufacture	coronary segment :AHA classification (n)
Multilink Plus	5	22	stainless steel	Guidant	#6(3), #7(1), #1(1)
Palmaz Schatz	1	25	stainless steel	J & J/Cordis	#7(1)
Tsunami	1	31	stainless steel	Terumo	#2(1)
BeStent2	1	33	stainless steel	Medtronic	#7(1)
NIR elite	4	37	stainless steel	Boston Scimed	#6(1), #13(1), #2(2)
Multilink Penta	16	49	stainless steel	Guidant	#6(5), #7(4), #1(1), #2(2), #3(4)
S670(S660)	20	50	stainless steel	Medtronic	#6(3), #7(5), #11(1), #13(1), #1(3), #2(4), #3(3)
Gfx	1	50	stainless steel	Medtronic	#6(1)
Express2	3	52	stainless steel	Boston Scimed	#6(1), #2(1), #11(1)
Tristar	1	55	stainless steel	Guidant	#3(1)
Cypher	3	55	stainless steel	J & J/Cordis	#7(3)
Driver	3	36	cobalt	Medtronic	#6(2), #2(1)
Cordis	1	50	tantalum	J & J/Cordis	#5(1)
Wiktor	1	50	tantalum	Medtronic	#1(1)

AHA, American Heart Association

Table 2

Results of the assessment of 61 coronary artery stents in patients by 16-slice MDCT

Stent diameter	Stent types(n)	Assessable stents	Non-assessable stents	The reasons for nonassessability : n (the stent types or the sites of stent implantation : AHA classification)
4.0mm n = 15	PL(1), NI(1), PE(5), S6(4), EX(2), DR(2)	14	1	(B) : 1 (#2)
3.5mm n = 22	PL(3), TS(1), NI(2), PE(4), S6(6), GF(1), TR(1), CY(1), DR(1), CO(1), WI(1)	17	5	(A) : 2 (CO, WI) (B) : 2 (#2, #2) (C) : 1 (#6)
3.0mm n = 19	PL(1), BE(1), NI(1), PE(6), S6(8), EX(1), CY(1)	11	8	(A) : 4 (BE, S6, S6, S6) (B) : 2 (#1, #3) (C) : 2 (#6, #6)
2.5mm n = 5	PS(1), PE(1), S6(2), CY(1)	0	5	(A) : 5 (PS, PE, S6, S6, CY)

The reasons for nonassessability : (A) partial volume effects and metal artifacts of stents, (B) banding artifacts (motion artifacts), (C) calcification.

Stent types : PL (Multilink Plus), PS (Palmaz Schatz), TS (Tsunami), BE (BeStent2), NI (NIR), PE (Multilink Penta), S6 (S670 or S660), GF (Gfx), EX (Express2), TR (Tristar), CY (Cypher), DR (Driver), CO (Cordis), WI (Wiktor).

Table 3
Assessability of S670 and Multilink Penta (diameter 3.5-mm, 3.0-mm), and the reasons for nonassessability

	S670	Multilink Penta
diameter 3.5mm	n=6 stents Assessable (n=5) Non-assessable (n=1) calcification (n=1)	n=4 stents Assessable (n=3) Non-assessable (n=1) banding artifact (n=1)
diameter 3.0mm	n=8 stents Assessable (n=3) Non-assessable (n=5) PVE and metal artifacts (n=3) banding artifact (n=2)	n=6 stents Assessable (n=4) Non-assessable (n=2) calcification (n=2)

S670 : coil stent, stainless steel, 0.0050inch.

Multilink Penta : tube stent, stainless steel, 0.0049inch.

PVE, partial volume effects

Fig 1

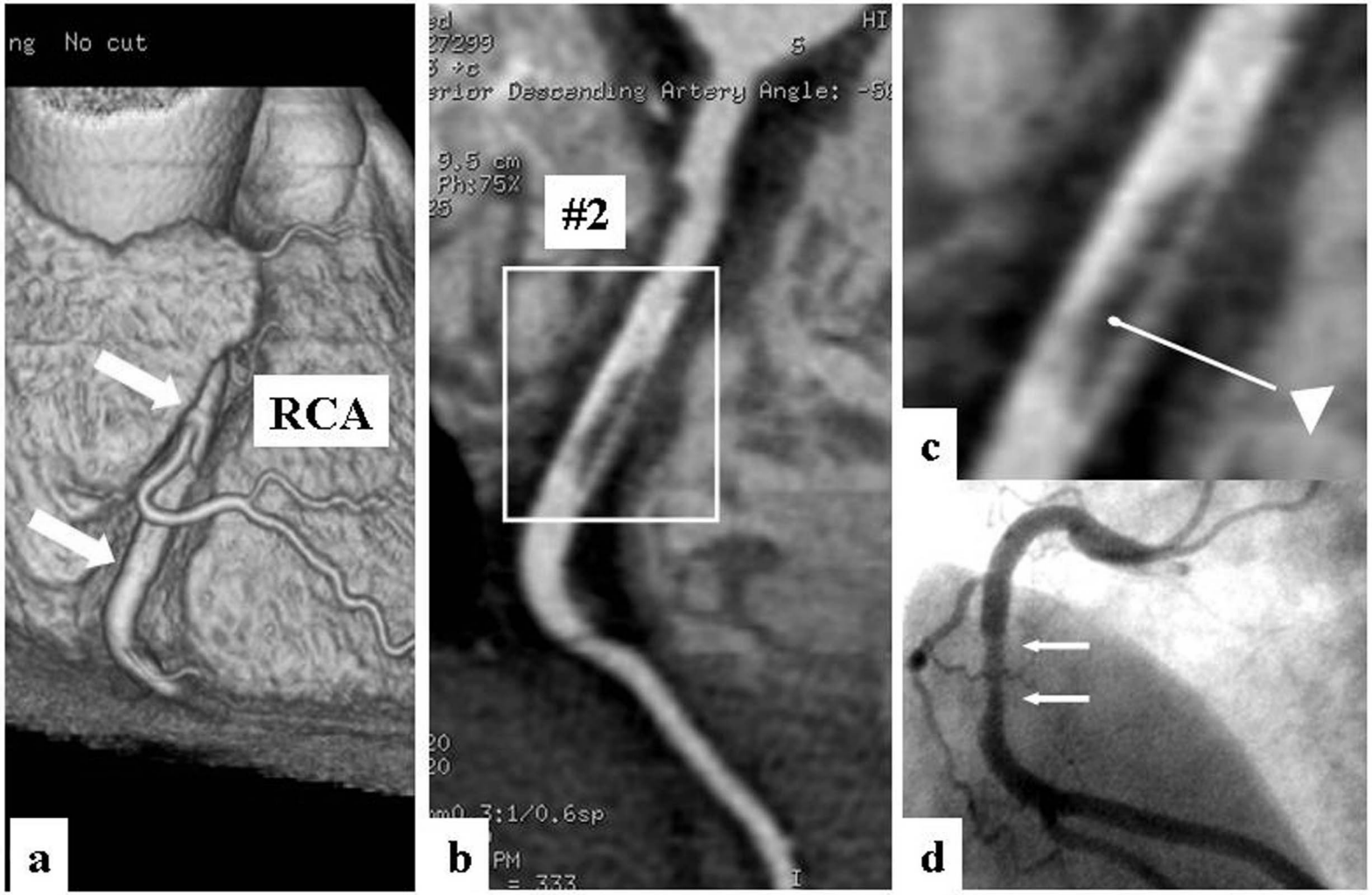

Fig 2

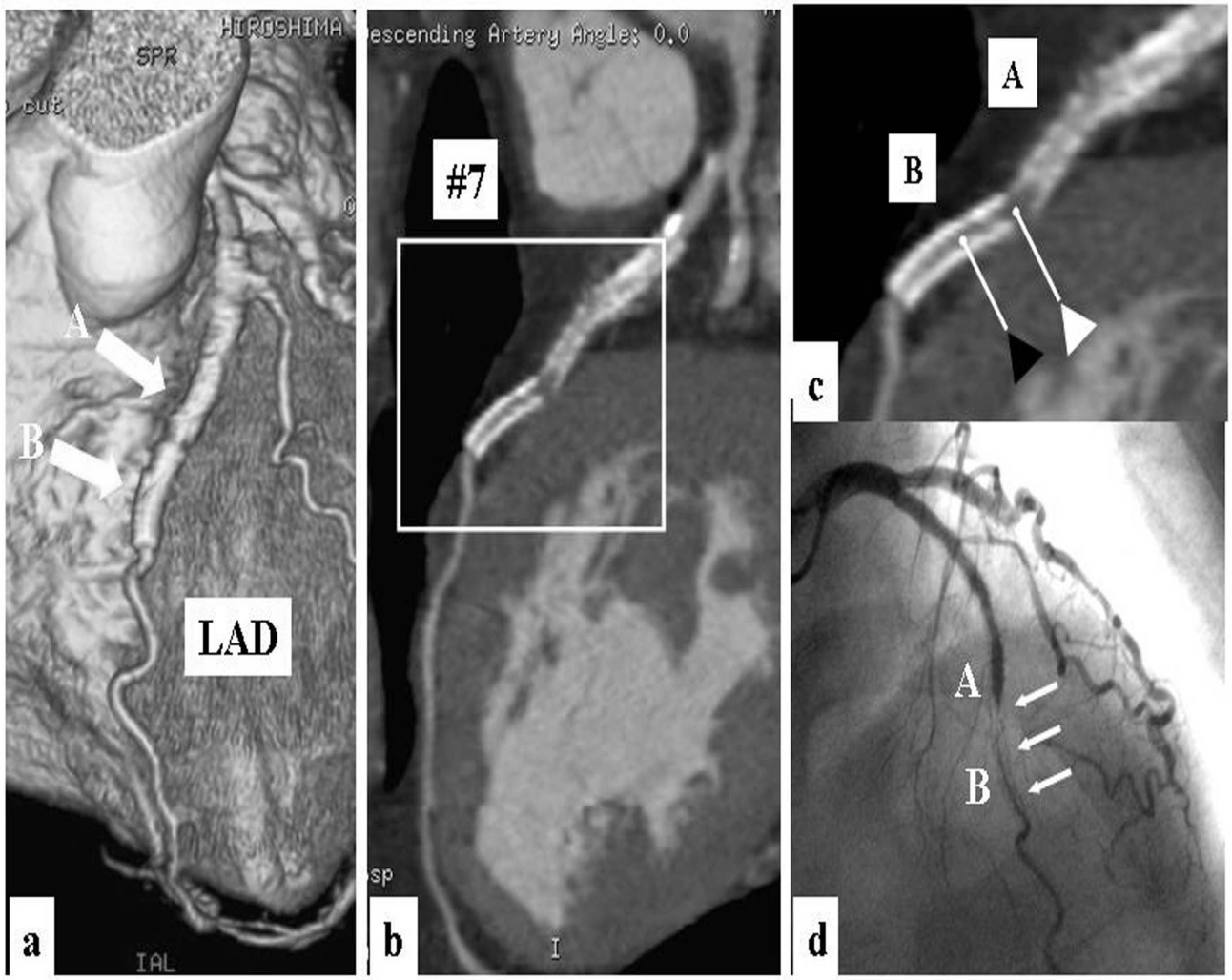

Fig 3